

# Template Polymerization of *N*-Vinylimidazole along Poly(methacrylic acid) in Water. 1. Influence of Template Concentration

H. T. van de Grampel, Y. Y. Tan,\* and G. Challa

Laboratory of Polymer Chemistry, Nijenborgh 16, 9747 AG Groningen, The Netherlands

Received March 23, 1990; Revised Manuscript Received May 16, 1990

**ABSTRACT:** The radical polymerization of *N*-vinylimidazole (VIm) was studied in the presence of hydrochloric acid (conventional polymerization), isobutyric acid (blank polymerization), and poly(methacrylic acid) (PMAA) (template polymerization) in aqueous solution at 50 °C. The conventional polymerization showed a deviation from normal kinetics above  $[VIm]_0 \approx 0.25$  M due to the presence of a so-called degradative addition of the radical to the monomer. This side reaction could be fully suppressed by decreasing the pH below 3, resulting in a rate increase. However, at  $[VIm]_0$  below 0.25 M, a pH reduction led to a decrease in rate. This was explained in terms of electrostatic repulsions between charged chain radicals and the protonated monomers. In the blank polymerization the degradative addition occurred above the higher  $[VIm]_0 \approx 0.45$  M, which is probably due to interactions of VIm with isobutyric acid. Template polymerizations were studied by using variable concentrations of PMAA at a constant  $[VIm]_0$  of 0.41 M. Rate enhancements with respect to the blank polymerization were observed up to a factor 6, beyond  $[PMAA]$  of 0.18 repeat unit mol/dm<sup>3</sup> (=baseM) only. A mechanism is proposed in which rate enhancements arise from the propagation of template-associated radicals with adsorbed mobile monomers. Complexation of these radicals with the template required the attainment of a critical number of electrostatic interactions, which was calculated.

## 1. Introduction

Template polymerizations can be defined as polymerizations in which polymer chains are able to grow along template macromolecules for the greater part of their lifetime. Such a mode of propagation can be achieved through the existence of cooperative interactions between the growing chain and the template chain and usually leads to the formation of an interpolymer complex. In general, a well-chosen template is able to affect the rate of polymerization as well as the molecular weight and microstructure of the formed polymer (daughter polymer).<sup>1</sup> The concepts of template polymerization were first described by Ballard and Bamford with the ring-opening polymerization of the *N*-carboxyanhydride of DL-phenylalanine on a polysarcosine template.<sup>2</sup> Since then, many other systems involving radical and nonradical initiation of vinyl monomers have been studied in which one or more template effects, arising from this peculiar propagation mode, were identified.<sup>1</sup> A number of radical-initiated template polymerizations have been studied, employing water as solvent.<sup>3-7</sup>

In our laboratory, only template polymerizations involving nonaqueous solutions have been studied in the past. The present system consisting of *N*-vinylimidazole (VIm) and poly(methacrylic acid) (PMAA) is the first one in aqueous solution.<sup>8</sup> The monomer VIm has not been used in template polymerization so far, though the kinetics of its conventional polymerization in EtOH, MeOH, and DMF has been described by various authors.<sup>9-16</sup> They found a deviation from classical kinetics with increasing monomer concentration, since the order in monomer and initiator inclined toward 0 and 1.0, respectively. This led to low rates of polymerization and low molecular weight polymers. On the basis of an extensive investigation in EtOH,<sup>9</sup> Bamford and Schofield concluded that these deviations could be attributed to a so-called degradative addition of the propagating radical to the imidazole ring at the 2-position, the resulting radical being stabilized by resonance structures. The polymerization in water at relatively high monomer concentrations showed an increase in  $R_p$  with decreasing pH.<sup>9</sup> It was proposed that the deg-

radative addition was impeded by protonation at the 3-position of the imidazole ring, since this would prevent resonance stabilization. Next to the determination of template effects, we were interested in whether the degradative addition could be suppressed by polymerization alongside the template, i.e., template polymerization.

A template effect is a polymer (chain) effect. To accentuate the latter, template polymerizations were compared with those using isobutyric acid (IBA) as a low molecular weight analogue of PMAA (further referred to as blank polymerization). Furthermore, the conventional polymerization of VIm in the absence of IBA was examined under template polymerization conditions to distinguish any influence of pH from template effects.

The choice of PMAA as template is related to the fact that the different stereoregular forms can be obtained easily. This is essential for studying the influence of the template microstructure on the template effects. In a series of papers we will discuss the use of linear atactic, syndiotactic, isotactic, and cross-linked PMAA as templates for the polymerization of *N*-vinylimidazole.

## 2. Experimental Section

**2.1. Materials.** *N*-Vinylimidazole (Aldrich) was distilled twice from CaSO<sub>4</sub> and stored at -18 °C. Isobutyric acid (Aldrich) was distilled once, and water was doubly distilled. The initiator 2,2'-azobis(2-amidinopropane)·2HCl (AAP; Polysciences) was used without further purification. AIBN was recrystallized from methanol.

Three samples of poly(methacrylic acid) were synthesized by a precipitation polymerization in toluene at 60 °C with benzoyl peroxide as initiator.<sup>17</sup> The polymers were repeatedly washed with diethyl ether to remove the toluene and dried at 50 °C under vacuum. The samples were kept in the vacuum desiccator in the presence of P<sub>2</sub>O<sub>5</sub>. Their viscosity-average molecular weights,  $M_v$ , were determined in methanol at 26 °C by using known  $K$  and  $a$  values.<sup>18</sup> The  $M_v$ 's were  $89 \times 10^3$  (PMAA-1),  $72 \times 10^3$  (PMAA-2), and  $88 \times 10^3$  (PMAA-3), respectively. PMAA-2 was used for the potentiometric measurements, PMAA-3 for the kinetic experiments with  $[AAP]_0 = 0.0235$  M, and PMAA-1 for all other experiments. The tacticity was determined of all samples by <sup>13</sup>C NMR as mm:mr:rr = 5:35:60.

Poly(*N*-vinylimidazole) was synthesized by polymerization of *N*-vinylimidazole in DMF at 70 °C under nitrogen with AIBN as initiator. The polymer was precipitated in acetone, dried, dissolved in ethanol, and reprecipitated in acetone.  $\bar{M}_v$  was determined in ethanol at 25 °C to be  $81 \times 10^3$  by using known  $K$  and  $a$  values.<sup>19</sup> Molecular weights of PVIm formed in the conventional polymerization were determined in 0.1 N HCl/1 M NaCl by a one-point viscometric measurement ( $c_p = 0.3$  g/dL) at 25 °C using known  $K$  and  $a$  values.<sup>42</sup>

**2.2. Polymerizations.** All polymerizations were performed at 50 °C with 2,2'-azobis(2-amidinopropane)·2HCl (AAP) as initiator. Its rate of decomposition in water at 60 °C is pH dependent but virtually constant within the range of pH 4–7.<sup>25</sup> It was assumed that this was also true at 50 °C.

Polymerizations were performed under nitrogen, which was purified by the usual methods. In a typical procedure for the template polymerization, VIm monomer and a solution containing PMAA and AAP were separately degassed by conventional freeze-thaw cycles until evolution of gas stopped. The aqueous solution was subsequently transferred to a thermostated reaction flask fitted with a nitrogen inlet and a Teflon stirrer at 50 °C. After temperature stabilization (less than 3 min), the monomer was injected into the reaction mixture.<sup>20</sup>

For the blank polymerization, PMAA was substituted by IBA. In the conventional polymerizations, the pH was adjusted by using degassed 5.0 M HCl or 5.0 M NaOH solutions. The conditions at pH  $8 \pm 0.2$  pH units refer to polymerizations of VIm, which were performed without adding HCl.

Monomer conversion for the template and conventional polymerizations was determined by means of UV measurements. Samples, diluted with water, were analyzed with UV by using the absorption maximum of VIm at 226 nm. The absorbance coefficient,  $\epsilon$ , was determined to be dependent on the pH according to  $\epsilon = 3403 + 1045\text{pH}$  (20 °C), the maximum value being 10 491 L/mol·cm.

Monomer conversion for the blank polymerization was determined by means of gas chromatography, since the UV absorption of IBA interfered with the absorption maximum of VIm. Each reaction sample was extracted with  $\text{CH}_2\text{Cl}_2$ , containing 2-octanol as internal reference, and injected into the gas chromatograph. The molar ratio of VIm to 2-octanol was compared with a calibration curve from which the amount of unconverted monomer in the reaction mixture could be deduced.

**2.3. Instrumental Methods.** Chromatographic analyses were performed by using a 9 ft  $\times$  8 in. column fitted with 10% Carbowax 20M Chrom WAW-DMCS (80–100 mesh) operating at 205 °C. UV measurements were performed with a Pye Unicam SP8-200 UV/vis spectrophotometer. Potentiometric measurements were carried out with a digital meter Digi 610 equipped with an Ingold combined electrode. <sup>13</sup>C NMR spectra were recorded at 75 MHz by using a Varian 300-MHz spectrometer. The tacticity was determined by using 10 wt % solutions in  $\text{D}_2\text{O}$ . Calorimetric experiments were performed with a Setaram Calvet type C80 twin microcalorimeter. Refractometric measurements were performed with an Atago refractometer. The refractive index was determined from solutions of IBA and VIm in various ratios while maintaining the total concentration of the two components at 0.8 M.

**2.4. Monomer Adsorption.** The percentage of adsorbed monomer was estimated by a combination of adsorption and desorption experiments in a Setaram microcalorimeter.<sup>21</sup> For the adsorption experiments, one compartment of the reaction cell contained an aqueous solution of VIm with  $[\text{VIm}] = 0.796$  M, and the other, a PMAA solution in water with  $[\text{PMAA}] = 0.785$  repeat unit mol/dm<sup>3</sup> (further denoted as baseM). For the desorption experiments, one compartment contained an aqueous solution of VIm and PMAA, and the other, only water. After the cell had attained thermal equilibrium (ca. 1.5 h) at 50 °C, the calorimeter was reversed several times in order to mix the solutions.

The experimental heat of an adsorption experiment,  $\Delta H_{\text{exptl}}$  is related to  $\theta$ , the degree of occupancy of the template, by  $\Delta H_{\text{exptl}} = \Delta H_s(\theta_j - \theta_i)$ , in which  $\Delta H_s$  is the molar heat of adsorption and the subscripts  $i$  and  $j$  signify conditions before and after mixing, respectively. The molar ratio of the heat of an adsorption ( $\theta_2, \theta_1$ )

**Table I**  
Heat Effects of Calorimetric Experiments

heat effect	change	value, <sup>a</sup> J/g solution
$\Delta H_{\text{adsorptn}}$		$-4.73 \pm 0.01$
$\Delta H_{\text{desorptn}}$		$0.549 \pm 0.003$
$\Delta H_{\text{ionizn}}(\text{PMAA})^b$	$\alpha_N = 0 \rightarrow \alpha_N = 0.45$	$-0.152$
$\Delta H_{\text{deprotonatn}}(\text{H}_2\text{O})^c$	pH 2.8 $\rightarrow$ pH 6.1	$0.117$
$\Delta H_{\text{protonatn}}(\text{VIm})$	$\alpha_N = 0 \rightarrow \alpha_N = 0.27$	$-2.72 \pm 0.07$

<sup>a</sup> End concentrations,  $[\text{VIm}] = 0.398$  M and  $[\text{PMAA}] = 0.393$  M.

<sup>b</sup> Reference 23. <sup>c</sup> Reference 22.

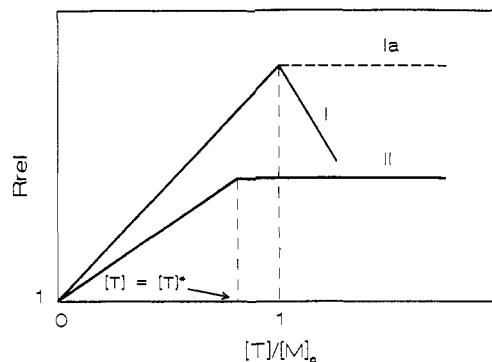


**Figure 1.** Schematic representation of kinetic curves for type I and type II template systems. Relative initial template polymerization rate,  $R_{\text{rel}}$ , versus  $[\text{T}]/[\text{M}]_0$  at constant  $[\text{M}]_0$ .

and desorption experiment ( $\theta_4, \theta_3$ ) can be written as

$$Z = \Delta H_{\text{exptl,a}} / \Delta H_{\text{exptl,d}} = (\theta_2 - \theta_1) / (\theta_4 - \theta_3)$$

If  $Z$  is determined under conditions chosen such that  $\theta_2 = \theta_3$  and  $\theta_1 = 0$ , then the equilibrium constant  $K_L$  for the conventional Langmuir-type adsorption can be solved by trial and error using the previous relationship and

$$\theta = ([\text{M}]_0 - [\text{M}_f]) / [\text{T}]_0 = K_L [\text{M}_f] / (1 + K_L [\text{M}_f])$$

with  $[\text{T}]_0$  the total template concentration in baseM and  $[\text{M}_f]$  and  $[\text{M}]_0$  the concentration of free monomer and total monomer concentration, respectively. In the case of VIm and PMAA, a correction had to be applied to the experimentally determined heat of complexation due to protonation and deprotonation processes, which occur upon mixing of the two solutions. Corrections were made for the deprotonation of water (endothermic),<sup>22</sup> increased ionization of PMAA (exothermic),<sup>23</sup> and protonation of VIm (exothermic). The molar heat of 100% protonation of VIm was determined by mixing a solution of VIm with a 1.0 N HCl solution and was  $25.6 \pm 0.2$  kJ/mol at 50 °C. The heat of dilution was negligible for these experiments. All relevant data are summarized in Table I.

Monomer adsorption was also determined by taking a sample from a solution of cross-linked PMAA and VIm at 50 °C, with  $[\text{VIm}] = 0.41$  M. The sample was analyzed by UV in the same way as described for the polymerization.

### 3. Theory of Template Polymerization

Template polymerizations can be divided into two idealized types depending on the strength of interactions between template and monomer.<sup>1</sup> A type I mechanism involves a strong specific interaction, leading to monomer preadsorption, whereas in a type II mechanism no interaction exists between template and monomer although interaction between the template and growing polymer develops. The specific mode of polymerization is usually inferred from kinetic studies in which the rate of polymerizations,  $R_p$ , is studied as a function of the template concentration ( $[\text{T}]$ ) at constant monomer concentration ( $[\text{M}]_0$ ).

The curves for the idealized mechanistic types I and II are depicted schematically in Figure 1, in which the relative rate,  $R_{\text{rel}} = R_p / R_{p,B}$  ( $R_{p,B}$  = blank rate) is plotted against

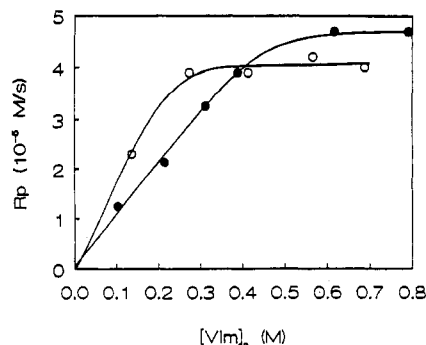


**Figure 2.** Rate of blank polymerization,  $R_p$ , as a function of  $[VIm]_0$  at  $[IBA]/[VIm]_0 = 1$  (curve a, ●) and conventional polymerization at pH 5.0 (curve b, ○);  $[AAP]_0 = 0.047$  M. Temperature = 50 °C.

$[T]/[M]_0$ . Curve I results when a type I mechanism is operative. Assuming a 1:1 interaction between the template unit and the monomer, the rate is maximal at a  $[T]/[M]_0$  of 1, i.e., when all the monomer is adsorbed on the template. When the template concentration is increased beyond this ratio, the degree of occupation and average length of monomer arrays decreases and the rate drops. However, if monomers are able to move along the template,  $R_{rel}$  will reduce less or even remain constant (curve Ia). Rate enhancements in a type I or Ia mechanism are thought to occur due to an increase in the propagation rate, caused by an elevated local monomer concentration, the ordering of monomer arrays, or suppression of monomer repulsion through adsorption on the template. Also, retardation of the termination step may contribute to the rate enhancement.

In a type II mechanism (curve II), preferential adsorption of monomer is absent and initial growth will start in the bulk solution. Complexation of the oligomeric radicals will occur only after attaining a critical chain length as a result of cooperative interactions. Polymerization then continues by adding monomer from the bulk solution, with rate enhancements resulting from retardation of the termination step. Provided that all oligomeric radicals are capable of complexing with the template chains, a maximal rate is attained at the critical overlap concentration, where the reaction volume is homogeneously occupied with template coils.

#### 4. Results and Discussion

**4.1. Blank Polymerization.** Blank polymerizations of VIm were performed in the presence of an equimolar quantity of IBA at a constant initial pH of 5. All conversion versus time curves were linear up to high conversions (>50%) as exemplified by curve d in Figure 8. The apparent zero-order plots may be explained by the occurrence of degradative addition.<sup>9-11</sup> A pH decrease of 0.2 units was observed between the beginning and the end of the polymerization. The small difference is caused by the higher  $pK_b$  of the formed polymer compared to that of the monomer and will be ignored. The  $\bar{M}_v$  of the resulting polymer was determined to be  $13.4 \times 10^3$  for  $[IBA] = 0.41$  M.

Rates of polymerization,  $R_p$ , were determined from the slopes of the initial linear parts of the conversion curves. The dependence of  $R_p$  on  $[VIm]_0$  is shown in Figure 2 (curve a), where it can be seen that  $R_p$  increases linearly up to  $[VIm]_0 \approx 0.45$  M, after which it becomes virtually constant. The order in monomer was determined from the slopes of  $\ln R_p$  vs  $\ln [VIm]_0$  and changed from  $0.95 \pm 0.05$  to  $0.1 \pm 0.07$  at ca. 0.45 M on increasing the monomer

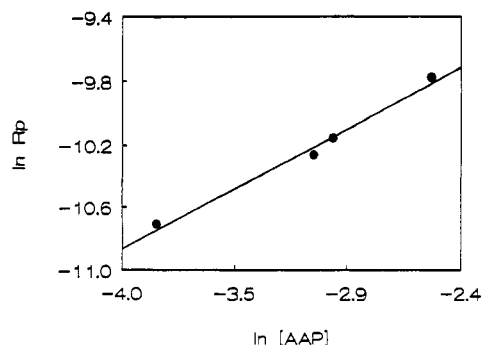


**Figure 3.**  $\ln R_p$  of blank polymerization versus  $\ln [AAP]_0$  at a constant  $[VIm]_0$  of 0.41 M and  $[IBA]/[VIm]_0 = 1$ . Temperature = 50 °C.

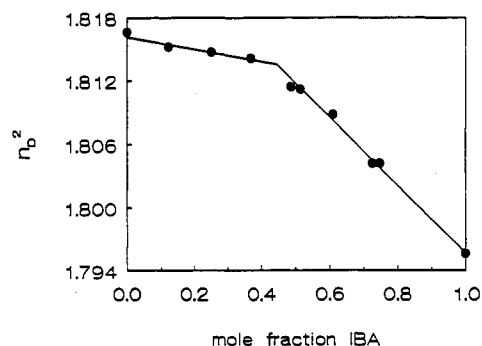


**Figure 4.** Refractometric data for aqueous solutions of IBA and VIm as a function of the mole fraction of IBA at  $([IBA] + [VIm]) = 0.8$  M. Temperature = 20 °C.

concentration. The approximately zero order beyond  $[VIm]_0 \approx 0.45$  M can be attributed to degradative addition.<sup>9-11</sup> At lower  $[VIm]_0$ , e.g., below 0.4 M, we expect classical kinetics in view of the monomer order of close to unity.

The order in initiator was determined for  $[VIM]_0 = 0.41$  M, the monomer concentration at which all template polymerizations were performed. At this concentration, however, the system seems to be a borderline case between classical and nonclassical kinetics as judged from Figure 2. Indeed, the order in  $[AAP]$  of  $0.75 \pm 0.1$ , which was calculated from the slope of  $\ln R_p$  vs  $\ln [AAP]_0$  (Figure 3), clearly points to the presence of degradative addition.

In order to determine the influence of IBA, the conventional polymerization of VIm was studied at pH 5. A similarly shaped plot as the one for the blank polymerization was obtained (Figure 2, curve b), with the degradative addition already occurring beyond  $[VIm]_0 \approx 0.25$  M. This is lower than the value of 0.45 M for the blank polymerization, which leads to the conclusion that IBA is able to partially suppress the degradative addition between  $[VIm]_0 = 0.25$  and 0.45 M. This is conceivable since it was reported<sup>24</sup> that low molecular weight additives are capable of influencing a polymerization by interaction with the monomer. Refractometric measurements of IBA-VIm mixtures indeed show a positive deviation from linearity (Figure 4), indicating interaction between VIm and IBA. This may also account for the fact that, at  $[VIm]_0$  below 0.45 M, the  $R_p$  is lower than the conventional polymerization rate, while above 0.45 M it is slightly higher.

**4.2. Conventional Polymerization.** It is known that the polymerization of VIm is sensitive not only to monomer concentration but also to pH changes.<sup>9</sup> This influence of pH was examined for two different concentrations: for a high  $[VIm]_0$  of 0.41 M where degradative addition is present and for a low  $[VIm]_0$  of 0.125 M where this side reaction is absent and classical kinetics is obeyed. It was

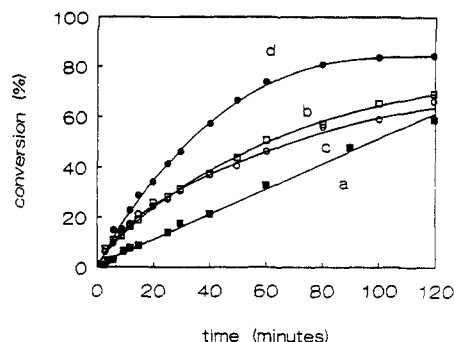


**Figure 5.** Conversion versus time plots for the polymerization of VIm as a function of pH.  $[VIm]_0 = 0.41$  M, pH 8 (curve a, ■) and pH 1 (curve b, □);  $[VIm]_0 = 0.125$  M, pH 1 (curve c, ○) and pH 8 (curve d, ●).

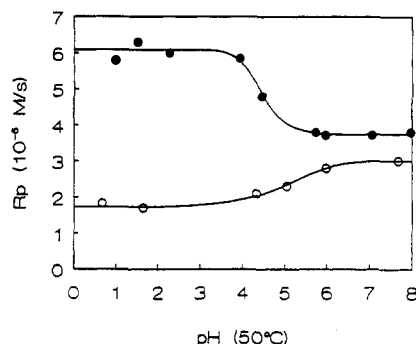


**Figure 6.** Rate of polymerization,  $R_p$ , as a function of pH (50 °C) at a constant  $[VIm]_0$  of 0.125 M (○) and 0.41 M (●).  $[AAP]_0 = 0.047$  M, temperature = 50 °C.<sup>38</sup>

expected that a decrease in pH would lead to a rate enhancement for  $[VIm]_0 = 0.41$  M, while the  $R_p$  at lower monomer concentrations would not be affected by the changing pH.

This different behavior is only partially reflected in the conversion curves (Figure 5). Indeed, linear conversion curves were obtained for  $[VIm]_0 = 0.41$  M at high pH (Figure 5, curve a), which is indicative of the degradative addition, while they were curved at low pH (Figure 5, curve b) and correspond better to classical kinetics. However, the conversion curves for  $[VIm]_0 = 0.125$  M obtained at pH 1 and 8, though both curved, obviously indicate different  $R_p$ 's (Figure 5, curves c and d).

The  $R_p$ 's are displayed in Figure 6 as function of pH. The striking difference between the two concentrations is obvious: for the high  $[VIm]_0$  the  $R_p$  nearly doubles with decreasing pH, while  $R_p$  decreases for the low  $[VIm]_0$ . In the first case, the rate increases on reduction of the pH from 7 to 3.5 (Figure 6), which coincides with an increase of the percentage of protonated VIm ( $VImH^+$ ) from 4% to 90%, respectively. This rate elevation can be attributed to suppression of degradative addition by protonation of the imidazole ring, as has been suggested by Bamford and Schofield.<sup>9</sup> This suppression is corroborated by the difference in shapes of the conversion curves obtained at high and low pH, respectively (Figure 5).

In the case of  $[VIm]_0 = 0.125$  M, protonation of the monomer leads to a 40% reduction of the  $R_p$  (Figure 6). Hence, the reactivity of  $VImH^+$  toward polymerization is smaller than that of the unprotonated monomer. This may be due to the electrostatic repulsion between two similarly charged particles (monomer and radical). Analogous behavior was found for the polymerization of MAA in water,<sup>27</sup> where  $R_p$  decreased with increasing pH.

The dual influence of pH was further elaborated by studying the influence of  $[VIm]_0$  at pH 8 and 1 (Figure

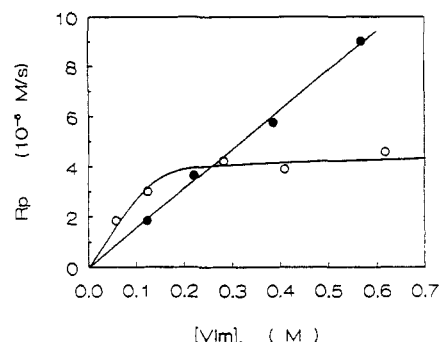


**Figure 7.** Rate of polymerization,  $R_p$ , as a function of  $[VIm]_0$  for pH 1 (●) and pH 8 (○).<sup>38</sup>

**Table II**  
Molecular Weights of PVIm Produced by the Conventional Polymerization

$[VIm]_0,^a$ M	$\bar{M}_v \times 10^3$	
	pH 1	pH 8
0.125	$9 \pm 1$	$13.5 \pm 1$
0.41	$16.5 \pm 1$	$10.5 \pm 1$

<sup>a</sup>  $[AAP]_0 = 0.047$  M.

7). At pH 8, the monomer is predominantly in the unprotonated state, while at pH 1 only protonated monomer molecules exist. The curve obtained for pH 8 is very similar to the curve obtained for pH 5 (Figure 2, curve b), since  $R_p$  is again zero order in monomer concentration beyond  $[VIm]_0 \approx 0.15$  M. On the other hand, the curve for pH 1 (Figure 7) is a straight line. The order in monomer (or rather in  $[VImH^+]$ ) was calculated to equal  $1.0 \pm 0.03$ , consistent with classical kinetics. The point of intersection of the two curves in Figure 7 yields the  $[VIm]_0$  whereby  $R_p$  is approximately independent of pH. At this concentration, the decrease of  $R_p$  due to VIm going to  $VImH^+$  is balanced by an increase in  $R_p$  resulting from a suppression of the degradative addition.

Molecular weights of the formed PVIm show a behavior nearly similar to the variation of pH (Table II). At pH 8, the slightly lower  $\bar{M}_v$  for  $[VIm]_0 = 0.41$  M compared to that for a  $[VIm]_0$  of 0.125 M corroborates the presence of degradative addition at the higher concentration.

**4.3. Monomer Adsorption.** The mode of propagation along the template as typified by the two ideal mechanisms can be estimated beforehand from the strength of the template-monomer interaction. This is usually derived from the degree of monomer preadsorption. Two techniques were used to determine this: UV spectroscopy and microcalorimetry.

For the spectrophotometric method, VIm was mixed with an aqueous solution of weakly cross-linked PMAA at 50 °C. From a sample taken from the supernatant solution, monomer adsorption at  $[VIm]_0 = 0.41$  M and  $[PMAA]/[VIm]_0 = 1.0$  was found to be  $25 \pm 3\%$ .

By using microcalorimetry<sup>21</sup> and assuming that adsorption of the monomer molecules by the template is of the Langmuir type, i.e., free template sites +  $VIm \xrightleftharpoons{K_L}$  occupied template sites in which  $K_L$  is the Langmuir adsorption coefficient, the amount of adsorbed monomer was  $43.5 \pm 0.4\%$ . The average value of 34% monomer adsorption, corresponding to a  $K_L$  of  $2 \text{ M}^{-1}$ , does not point to either of the ideal systems.

**4.4. Template Polymerization.** Typical conversion versus time curves obtained for three  $[PMAA]$  at a constant  $[VIm]_0$  of 0.41 M are shown in Figure 8. All conversion curves obtained for  $[PMAA]_0 < 0.18$  baseM were linear as exemplified by curve a in Figure 8. This linearity was

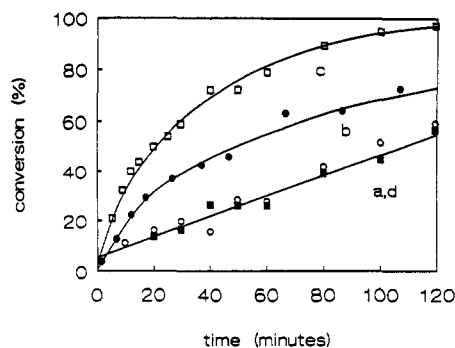


**Figure 8.** Conversion versus time plots for three template polymerizations of VIm along atactic PMAA at a constant  $[VIm]_0$  of 0.41 M and  $[AAP]_0 = 0.047$  M.  $[PMAA] = 0.18$  (curve a,  $\circ$ ),  $[PMAA] = 0.34$  (curve b,  $\bullet$ ), and  $[PMAA] = 0.41$  baseM (curve c,  $\square$ ). A blank polymerization of VIm in the presence of  $[IBA] = 0.41$  M is shown for comparison (curve d,  $\blacksquare$ ).

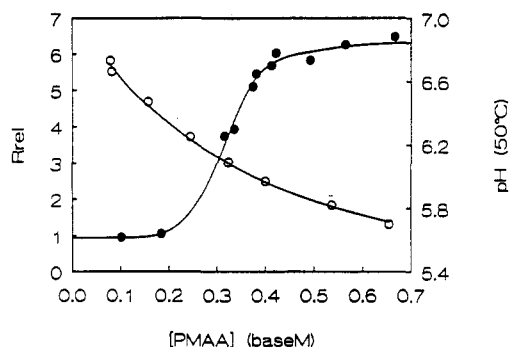


**Figure 9.** Relative rate of template polymerization,  $R_{rel}$  ( $\bullet$ ), versus  $[PMAA]$  and  $pH(50^\circ C)$  ( $\circ$ ) of initial reaction mixtures without AAP versus  $[PMAA]$ .  $[VIm]_0 = 0.41$  M,  $[AAP]_0 = 0.047$  M. Temperature =  $50^\circ C$ .

also encountered at the blank polymerization (curve d). The initial  $R_p$  was calculated from conversion vs time ( $\alpha$  vs  $t$ ) plots and was also equal to the blank rate.

At  $[PMAA]_0 > 0.18$  baseM, the conversion curves assumed normal first-order shapes as is demonstrated by curves b and c in Figure 8. The  $R_p$  was calculated from linear  $-\ln(1 - \alpha)$  vs  $t$  curves, using first-order kinetics<sup>28</sup> to avoid extrapolation errors in determining  $d\alpha/dt$  at low conversions.

Template polymerizations, which were performed at  $[PMAA] > 0.18$  baseM, became heterogeneous with time and eventually resulted in the separation of a solid complex between PMAA and PVIm as determined by NMR and elemental analysis. At lower PMAA concentrations, only a small amount of transparent sticky material was produced, which probably consisted of loosely complexed PVIm with PMAA.

In Figure 9, the relative rate of polymerization,  $R_{rel}$ , is plotted versus  $[PMAA]$  at a constant  $[VIm]_0$  of 0.41 M. Three regions can be discerned, i.e., region A at  $[PMAA] < 0.18$  baseM with no rate enhancements, region B at  $0.18 < [PMAA] < 0.41$  baseM with a rapid increase in  $R_{rel}$ , and region C at  $[PMAA] > 0.41$  baseM with an almost constant but elevated rate.

In view of the pH dependency of the rate in the conventional polymerization of VIm, the pH is also plotted in Figure 9. The gradual decrease of the pH shows no abnormalities from pH 6.7 (at  $[PMAA] = 0.1$  baseM) to pH 5.7 (at  $[PMAA] = 0.68$  baseM). In this pH range, the rate of the conventional polymerization is invariant (Figure 6) as well as the  $k_d$  of AAP.<sup>25</sup> Therefore, we can safely conclude that the profile of the curve in Figure 9 is not related to the pH sensitivity of either the conventional polymerization of VIm or the decomposition rate of AAP.

At this point it should be remarked that the pH of the bulk solution differs from the local pH in the vicinity of the template chain. Since our template polymerization comprises pH-sensitive reactions in bulk solution as well as near the template, both values are important. The local pH should be lower than the bulk pH due to an enhanced electrostatic potential of the charged polyanion. This creates a cylindrical double layer around the template with an ionic strength higher than the bulk solution.<sup>40</sup> Several methods are known to determine the electrostatic potential and its influence upon the local pH and ion concentrations, e.g., by numerically solving the Poisson-Boltzmann equation<sup>40</sup> or by using pH-sensitive chromophores covalently attached to the polymer chain.<sup>41</sup> If applied to this case, additional complications arise due to the presence of unknown quantities of VIm, protonated VIm, and positively charged AAP near the template at different  $[PMAA]$ .

If one considers the possible impact of a lower local pH, one may expect that the rate of the conventional polymerization in the double layer around the template might be higher compared to that of the bulk solution (see Figure 6). Its contribution to the overall rate, however, may be neglected since the residence time of a radical in the double layer prior to its complexation is relatively short. Also, the influence of local pH on the dissociation of AAP is negligible since its dissociation constant is not affected between pH 4 and 7 and is only slightly raised at pH < 4. However, the positively charged AAP will interact with the template, leading to initiation close to the chain and the possibility of primary termination of template-associated radicals. For the present the only obvious effect of a lower local pH will be an elevated concentration of protonated monomer molecules and initiator ions in the vicinity of the chain.

**AB Transition.** In order to understand the above results the two transitions AB and BC need clarification. In region A, there is obviously no template effect. Moreover, no precipitate due to complex formation was observed during polymerization. Evidently, PVIm radicals, which initially propagate in solution, are prematurely terminated due to the degradative addition to monomer, rendering them unable to associate with the template.

In region B, rate enhancements are accompanied by non-linear conversion curves, which follow normal kinetics.<sup>28</sup> Furthermore, precipitates were produced during polymerization, indicating that PVIm radicals were able to form complexes with the template chains and continue their growth alongside the templates. The strong rise in  $R_{rel}$  in region B may be explained by growth of these template-associated radicals, since rate enhancements will result from (1) retardation of the termination step, (2) suppression of the degradative addition to monomer through propagation of predominantly protonated (adsorbed) monomer, and (3) a reduction of electrostatic repulsions between the propagating charged radical and protonated monomer due to their interactions with the template. The latter was suggested by Tsuchida et al. in the polymerization of methacrylic and acrylic acid in the presence of ionenes in aqueous solution.<sup>3</sup>

The question arises as to why complexation between PVIm and PMAA starts at the AB transition. Complexation between two complementary nonionic polymers with monomeric units equivalent to an interaction site should be determined by the cooperativity principle.<sup>29,35</sup> This principle states that complexation is possible when the sum of the enthalpies of  $n$  interactions exceeds the losses of entropy of the chains. Since the largest entropy loss of

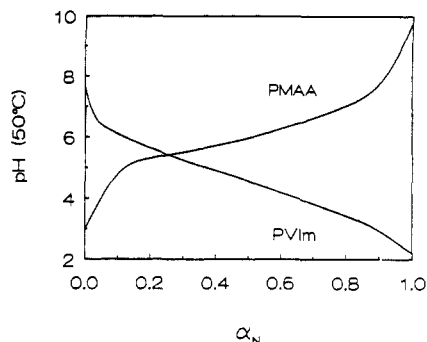


**Figure 10.** Potentiometric titration curves of PVIm ( $c_p = 3.6$  g/dL) and PMAA ( $c_p = 3.19$  g/dL) in water at 50 °C with 1.0 N HCl and 1.0 N NaOH, respectively.

the polymer chains results from the first interaction and the energy of each interaction remains virtually constant, complexation becomes more feasible as  $n$  increases. The critical number of interactions,  $n^*$ , corresponding to the occurrence of complexation is then called the critical chain length,  $l^*$ .

In the case of complexation between a weak polyacid and a weak polybase, the mode of interaction (hydrogen bonding or electrostatic) and  $n$  are determined by the degrees of ionization of the two constituent polymers, which can be varied by changing the pH.<sup>29,32</sup> The critical chain length,  $l^*$ , is then determined not only by the chain length,  $l$ , but also by the charge density,  $\rho$ . Complexation can be effected by either of the two variables. We will examine to what extent  $l$  and  $\rho$  are affected by changing pH.

In the case of PVIm and PMAA, let us first consider which interaction forces influence primary complexation. Complexation is thought to occur via both electrostatic interactions and hydrogen bonds; i.e.,  $n$  can be written as  $n = n_{el} + n_{hb}$ , with  $n_{el}$  the number of electrostatic interactions and  $n_{hb}$  the number of hydrogen bonds. Hydrophobic interaction may stabilize the complex, although it may also influence the conformation of PMAA.<sup>30</sup>

At low degrees of neutralization PMAA has a contracted conformation due to hydrophobic interaction between the methyl groups counteracting the expanding force exercised by the electrostatic repulsions between the  $\text{COO}^-$  groups. Since complex stability and composition are dependent on the accessibility of interaction sites, it was determined whether or not hydrophobic interaction influenced primary complexation. The potentiometric titration curves for both polymers are shown in Figure 10. The compact conformation of PMAA is evidenced by the deviation of the curve at low  $\alpha_N$ . The deviation is surprisingly small since the high temperature should have led to an increased hydrophobic interaction. Template polymerizations were performed within the pH range from 6.66 to 5.7, corresponding to  $\alpha_N$  between 68 and 40%. This is well above the  $\alpha_N$  of 35%, below which hydrophobic interactions start to influence the conformation of PMAA.<sup>30</sup> It is known that PVIm has no conformational transition in aqueous solution on titration with HCl.<sup>31</sup> Nevertheless, the small deviation at low  $\alpha_N$  seems to point to a stabilized compact conformation at  $\alpha_N$  below ca. 0.04. This deviation, albeit smaller, was also found by Henrichs et al.<sup>31</sup> Their viscometric measurements did not reveal a conformational transition, though a compact conformation of PVIm was observed at high ionic strength due to intramolecular hydrogen bonds. The more pronounced deviation in our case may be caused by the higher temperature (50 °C) and polymer concentration. Since the deviation is slight, it is

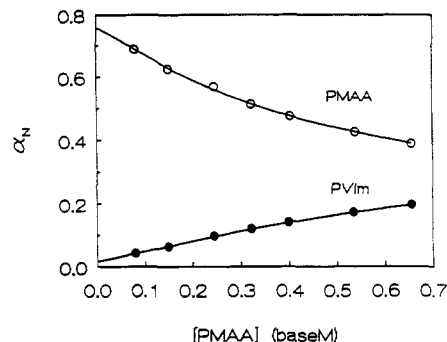


**Figure 11.** Degree of neutralization,  $\alpha_N$ , of PVIm ( $c_p = 3.6$  g/dL) and PMAA ( $c_p = 3.19$  g/dL) versus [PMAA] as calculated from Figures 9 and 10.

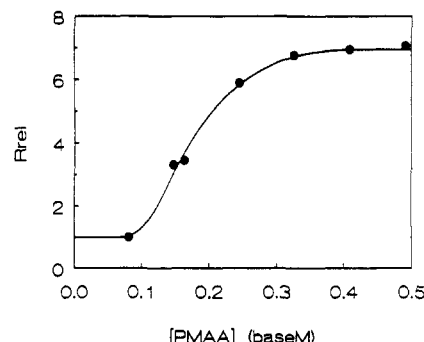


**Figure 12.** Relative rate of template polymerization,  $R_{rel}$ , versus [PMAA] at a constant  $[\text{VIm}]_0$  of 0.41 M and  $[\text{AAP}]_0$  of 0.024 M. Temperature = 50 °C.

unlikely that this would affect complexation between PVIm and PMAA.

Consequently, complexation is achieved by a changing  $l$  and/or  $\rho$ . Assuming a constant mode of termination, e.g., predominantly degradative addition to monomer, the average chain length of the radicals ( $l$ ) in solution would hardly alter over the whole range of [PMAA] (A–C), since the gradual reduction of pH in this range does not appreciably influence the conventional polymerization (see Figure 6). Thus, a changing  $l$  can be dismissed as a cause for inducing complexation at the AB transition.

However, the gradual reduction of pH in region A leads to a significant change in the charge density of the PVIm radicals. In Figure 11,  $\alpha_N$  is plotted against [PMAA] as derived from Figures 9 and 10. In region A, the  $\alpha_N$  of PMAA decreases slightly from 68 to 60%, but the  $\alpha_N$  of PVIm increases from 4.3 to 8.9%. The latter leads to an increase in the number of potential electrostatic interactions ( $n_{el}$ ) between a PVIm radical and PMAA by a factor of 2, while  $n_{hb}$  hardly varies. Accordingly, the association ability of the radical with the template is increased. In other words, radicals reach  $l^*$  at the AB transition, where the critical amount of interactions,  $n^*$ , necessary to form a complex with PMAA is attained. The essential role of  $l^*$  of the PVIm radical is further demonstrated by the fact that, upon reduction of the initiator concentration to half its value (Figure 12), the AB transition shifted from [PMAA] of 0.18 to the lower value of 0.09 baseM. The decreased initiator concentration leads to longer radicals, which are then able to complex with the template at a lower charge density. This is achieved at a higher pH, i.e., a lower template concentration.

Furthermore,  $l^*$  will become shorter as the charge density of the radicals increases with [PMAA], eventually enabling all radicals to complex with the template before termination occurs.



Some literature data are provided for  $n^*$ , the critical amount of interactions necessary for complexation, which equaled  $l^*$  in all cases.<sup>29,33,34</sup> A value of 4 was obtained for  $n^*$  for the complexation of quaternized oligo(ethylenimine) with PMAA in water (electrostatic interaction)<sup>33</sup> and 40 for poly(ethylene oxide) with PMAA (hydrogen bonding).<sup>34</sup> Clearly,  $n_{el}$  is much smaller than  $n_{hb}$  because of the weaker hydrogen bonding.

To estimate  $n_{el}$  in our case we assume that (1)  $\bar{P}_v = 2\bar{P}_n$ , (2) termination by degradative addition predominates, and (3)  $n_{hb}$  is negligible since only  $n_{el}$  changes at the AB transition. Also, conformational aspects are ignored since it is not possible to estimate the loss of entropy on complexation of a PVIIm radical with PMAA. The  $\bar{M}_v$  of the polymers obtained in the blank polymerization was ca.  $13.4 \times 10^3$ , leading to an average length of 71 monomer units for the radicals. When it is known that at the AB transition the  $\alpha_N$  of PVIIm equaled 8.9% (Figure 11), a value of 6 charges per PVIIm radical on complexation was calculated, which is comparable to the literature data. The same procedure was applied to the AB transition in Figure 12, where half the  $[AAP]_0$  was used and rate enhancements started to occur at  $[PMAA] = 0.09$  baseM. An average length of 142 monomer units for the radical was estimated, which also leads to a  $n_{el}$  of 6. This value is remarkably similar to the previous value obtained for  $[AAP]_0 = 0.047$  M, especially if one takes account of the greater potential for hydrogen bonding at longer chain lengths. Complexation experiments are now being done to study  $n_{el}$  more extensively.

**BC Transition.** Finally, we will discuss the BC transition where  $R_p$  levels off. At this point, which corresponds to a  $[PMAA]/[VIm]_0$  of 1, no abrupt changes in the potentiometric titration curves (Figure 10) or  $\alpha_N$  of either polymer occurred (Figure 11). Consequently, this transition may either be explained by the attainment of a critical overlap concentration (type II mechanism) or a maximal "zipping-up" rate along the template chain (type I mechanism).

A critical overlap concentration for polyelectrolytes in aqueous solution is generally hard to define due to the charges they carry. PMAA, on the other hand, is a weak polyelectrolyte and thus hardly ionizes in water, so the existence of a possible overlap concentration was verified. The overlap concentration for aqueous solutions of PMAA-1 in the absence of salt was determined to be 3.2 g/dL, with the ionization of PMAA below 5%.

Under template polymerization conditions, however, with pH ranging from 5.7 to 6.66, the  $\alpha_N$  of PMAA is 40–68% and, consequently, PMAA has a much more expanded conformation. Overlap would occur at much lower concentrations than 3.2 g/dL, though electrostatic repulsions between the similarly charged coils would seriously hamper overlap.<sup>39</sup> Furthermore, the BC transition was shifted when a lower initiator concentration was used (Figures 9 and 12). Therefore, the existence of a critical overlap concentration in a type II mechanism can be ruled out as the cause for the BC transition. A pure type II mechanism would be in contradiction with the preferential monomer adsorption by the template.

This leaves a type I mechanism with a maximum  $R_p$  at  $[PMAA]/[VIm]_0$  of unity (see Figure 1). This mechanism requires, however, that all radicals and monomer molecules are adsorbed on the template chains at and beyond a  $[PMAA]/[VIm]_0$  of 1. If the adsorbed monomer molecules were immobile (site-bound),  $R_p$  would decrease beyond a  $[PMAA]/[VIm]_0$  of 1; if on the other hand monomer molecules were mobile,  $R_p$  would remain constant (type

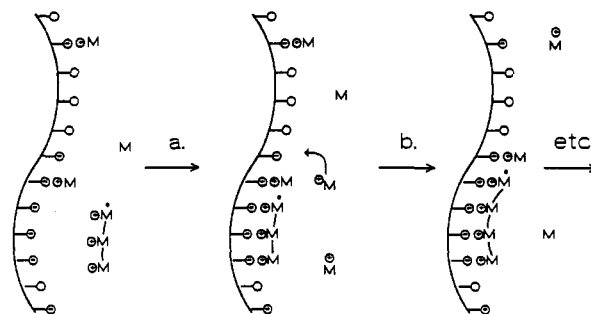


**Figure 13.** Schematic representation of the propagation process at the template chain: step a, complexation of a radical with the template; step b, movement of a monomer molecule along the chain; and a propagation step.

Ia in Figure 1). The obtained rate profile clearly points to the latter. However, refinement of a type Ia mechanism is necessary since we are dealing with a limited preferential adsorption of monomer (ca. 34%). A maximum  $R_p$  will be obtained if the propagation rate is the rate-limiting process taking place at the template chain. This means that as long as monomer molecules are sufficiently mobile to fill the empty template site next to the associated chain radicals before propagation occurs, the rate will be independent of the amount of monomer adsorbed on the template. A polymerization mechanism in the B and C region is now proposed, taking into account the following considerations:

(1) All radicals in solution will complex with the template chains after attaining  $l^*$  (region B). This assumes that termination or degradative addition in solution is of minor importance or completely absent.

(2) Although only ca. 34% of the monomer molecules are adsorbed onto the template, the inherent mobility of the monomers along the template chain is strongly enhanced through rapid adsorption/desorption equilibria, which run parallel with protonation/deprotonation processes.

(3) Propagation is the rate-limiting step in the process along the template chain.

The propagation steps of the polymerization process are visualized in Figure 13. After  $l^*$ , the critical chain length at which the radical is capable of  $n^*$  interactions necessary to form a complex is attained, the PVIIm radical will complex with the template (Figure 13, step a). Polymerization then continues by adding adsorbed monomer molecules (Figure 13, step b), which can adsorb in two ways, i.e., an uncharged monomer at a COOH site or a charged monomer at a COO<sup>-</sup> site. Only the last adsorption mode is depicted. The high local concentration of monomers in the vicinity of the template chain due to the high local ionic strength characteristic of polyelectrolytes may further contribute to the observed rate enhancement. The uninterrupted propagation of the radical is illustrated by step b in Figure 13 in which a monomer is being adsorbed next to the monomer that is about to be added to the radical. Whether or not monomer addition by the radical occurs simultaneously with adsorption is not very important as long as monomer is available for propagation. The system can be viewed as being homogeneously occupied by template chains. It is thought that at the end of a template chain, radicals can "hop" to a next template chain to continue their propagation.<sup>36</sup>

The mode of termination of the growing template-associated radical, i.e., with another template-associated radical or with a radical in solution, has not been mentioned so far but will be discussed in a next paper in which the

molecular weights of the template-formed PVIm were studied.

The position of the BC transition for the experiments with half  $[AAP]_0$  (Figure 12) appeared at a lower  $[PMAA]/[VIm]_0$  than unity. This shift is probably caused by the fact that all radicals became complexed with the template at a lower  $[PMAA]$  due to their greater length, rendering the above-described mechanism (Figure 13) possible at a lower  $[PMAA]$ . The difference in maximal rate enhancement can be explained by the lower concentration of template-associated radicals, which further retards termination.<sup>37</sup>

## 5. Conclusion

In this paper we have demonstrated that in conventional polymerization a side reaction occurred at  $[VIm]_0 \approx 0.25$  M at 50 °C. This degradative addition to monomer could be suppressed by the polymerization of protonated monomers, i.e., by decreasing the pH below pH 3. However, at these low pH values, electrostatic repulsions between protonated monomers and radicals caused a decrease in  $R_p$ . Blank polymerization of VIm in the presence of IBA led to lower  $R_p$ 's, but the degradative addition was found to occur above the higher  $[VIm]_0$  of 0.45 M. This can be attributed to interactions between IBA and VIm.

The degradative addition could also be suppressed by template polymerization, as was evidenced by rate enhancements. Moreover, since the suppression of the degradative addition can only lead to a rate enhancement by a factor 1.9, the greater part of the rate enhancement has to be attributed to template effects, i.e., a retardation of the termination step through loss of mobility of the radicals on association with the template. The reduction of electrostatic repulsions between the propagating radical and adsorbed monomers due to association with the template may also contribute to the increase in  $R_p$ .

Essential for a template effect in this case appeared to be the ability of a radical chain to complex with the template as measured by  $n^*$ , the number of interactions necessary to achieve complexation. The chain length at which  $n^*$  is attained could be influenced by the pH and initiator concentration. The propagation process of template-associated radicals could be described by a modified type I polymerization in which adsorption of monomers precedes polymerization.

**Acknowledgment.** This study was supported by the Netherlands Foundation for Chemical Research (SON) with financial aid from the Netherlands Organization for Scientific Research (NWO). We thank Ms. L. van de Vegt for performing the blank polymerizations.

## References and Notes

- (1) Tan, Y. Y.; Challa, G. *Encycl. Polym. Sci. Eng.* **1989**, *16*, 554.
- (2) Ballard, D. G. H.; Bamford, C. H. *Proc. R. Soc. London* **1956**, *A236*, 384, 495.
- (3) Tsuchida, E.; Osada, Y. *J. Polym. Sci., Polym. Chem. Ed.* **1975**, *13*, 559.
- (4) Sato, T.; Nemoto, K.; Mori, S.; Otsu, T. *Macromol. Sci.* **1979**, *A13*, 751.
- (5) Ferguson, J.; Al-Alawi, S.; Granmayeh, R. *Eur. Polym. J.* **1983**, *19*, 475. Ferguson, J.; Shah, S. A. O. *Ibid.* **1968**, *4*, 611. Ferguson, J.; Eboatu, A. *Ibid.* **1989**, *25*, 731.
- (6) Klein, C. *Makromol. Chem.* **1972**, *161*, 85.
- (7) Blumstein, A.; Weill, G. *Macromolecules* **1977**, *10*, 75.
- (8) Van de Grampel, H. T.; Tan, Y. Y.; Challa, G. *Makromol. Chem., Macromol. Symp.* **1988**, *20/21*, 83.
- (9) Bamford, C. H.; Schofield, E. *Polymer* **1981**, *22*, 1227.
- (10) Bamford, C. H.; Schofield, E. *Polym. Commun.* **1983**, *24*, 4.
- (11) Bamford, C. H.; Schofield, E. *Polymer* **1983**, *24*, 433.
- (12) Joshi, M. G.; Rodriguez, F. *J. Appl. Polym. Sci.* **1984**, *29*, 1345.
- (13) Dambatta, B. B.; Ebdon, J. R. *Eur. Polym. J.* **1986**, *22*, 783.
- (14) Konsulov, V. B.; Wolff, L. A.; Shwetz, N. V.; Domnina, E. S.; Skvortsova, G. G. *Isv. Uchebn. Zaved. Khim. Tekhnol.* **1976**, *19*, 1263; *Chem. Abstr.* **1976**, *85*, 160649b.
- (15) Shusnikova, A. I.; Domnina, E. S.; Skvortsova, G. G. *Vysokomol. Soedin. Ser. B*, **1977**, *19*, 372; *Chem. Abstr.* **1977**, *87*, 39919c.
- (16) Konsulov, V. B. *Dokl. Bolg. Akad. Nauk.*, **1978**, *31*, 1305; *Chem. Abstr.* **1979**, *90*, 152682v.
- (17) Bartels, T.; Tan, Y. Y.; Challa, G. *J. Polym. Sci., Polym. Chem. Ed.* **1977**, *15*, 341.
- (18) Wiederhorn, N. N.; Brown, A. M. *J. Polym. Sci.* **1952**, *8*, 651.
- (19) Eskin, V. Ye.; Magasik, S. Y.; Zhurayev, U. B.; Rudkovskaya, G. D. *Polym. Sci. USSR* **1978**, *20*, 2494.
- (20) A solution containing PMAA and VIm is very viscous due to the expanded conformation of PMAA at pH 6. Injection of a solution of AAP to such a viscous reaction mixture would hamper rapid mixing of the components.
- (21) Smid, J. Ph.D. thesis, Groningen, 1981; *Eur. Polym. J.* **1984**, *20*, 887, 1095; *Ibid.* **1985**, *21*, 141.
- (22) Hepler, L. G.; Woodley, E. M. In *Water, A Comprehensive Treatise*; Franks, F., Ed.; Plenum Press: New York, 1973; Vol. 3, Chapter 3.
- (23) Crescenzi, V.; Delben, F.; Quadrifoglio, F.; Dolar, D. *J. Phys. Chem.* **1973**, *77*, 539. Crescenzi, V.; Delben, F.; Quadrifoglio, F. *J. Polym. Sci., Polym. Phys. Ed.* **1972**, *10*, 357.
- (24) Kabanov, V. A.; Topchiev, D. A.; Karaputadze, T. M. *J. Polym. Sci., Polym. Symp.* **1973**, *42*, 173. Kabanov, V. A.; Topchiev, D. A.; Karaputadze, T. M.; Mkrtchian, L. A. *Eur. Polym. J.* **1975**, *11*, 153.
- (25) Ito, K. *J. Polym. Sci., Polym. Chem. Ed.* **1973**, *11*, 1673.
- (26) This was calculated from the  $pK_a$  of VIm, which was determined from potentiometric titrations to be 5.52 at 50 °C.
- (27) Katchalsky, A.; Bauer, G. *Trans. Faraday Soc.* **1951**, *47*, 1360.
- (28) The dependence of  $R_p$  on monomer and initiator concentration was measured for  $[VIm]_0 = 0.41$  M and  $[PMAA]/[VIm]_0 = 1$  and showed normal kinetics with first order and nearly half order dependencies in monomer and initiator concentrations, respectively. This will be published in a subsequent paper.
- (29) Tsuchida, E.; Abe, K. *Adv. Polym. Sci.* **1982**, *45*, 1.
- (30) Bekturov, E. A.; Bakanova, Z. Kh. In *Synthetic water-soluble polymers in solution*; Huthig & Wepf: Basel, Switzerland, 1986.
- (31) Henrichs, P. M.; Whitlock, L. R.; Sochor, A. R.; Tan, J. S. *Macromolecules* **1980**, *13*, 1375.
- (32) Abe, K.; Koide, M.; Tsuchida, E. *Macromolecules* **1977**, *10*, 1259.
- (33) Tsuchida, E.; Osada, Y. *Makromol. Chem.* **1974**, *175*, 593.
- (34) Ikawa, T.; Abe, K.; Honda, K.; Tsuchida, E. *J. Polym. Sci., Polym. Chem. Ed.* **1975**, *13*, 1505.
- (35) Papisov, I. M.; Litmanovich, A. A. *Adv. Polym. Sci.* **1988**, *90*, 139.
- (36) Gons, J.; Straatman, L. J. P.; Challa, G. *J. Polym. Sci., Polym. Chem. Ed.* **1978**, *16*, 427.
- (37) Tan, Y. Y.; Alberda van Ekenstein, G. A. accepted for publication in *Macromolecules*.
- (38) All values have been corrected for the pH dependence of the dissociation constant of AAP at high and low pH values by using data obtained by Ito.<sup>25</sup>
- (39) Mandel, M. *Encycl. Polym. Sci. Eng.* **1988**, *15*, 795-799 and references therein.
- (40) Oosawa, F. *Polyelectrolytes*; Marcel Dekker: New York, 1971.
- (41) Ishikiwa, M. *Macromolecules* **1979**, *12*, 498 and 502.
- (42) Morishima, Y.; Kobayashi, T.; Nozakura, S. *Macromolecules* **1988**, *21*, 101. Fernandez, M. S.; Fromherz, P. *J. Phys. Chem.* **1977**, *81*, 1755.
- (42) Tan, J. S.; Sochor, A. R. *Macromolecules* **1981**, *14*, 1700.

**Registry No.** VIm, 1072-63-5; PMAA, 9011-14-7; HCl, 7647-01-0; isobutyric acid, 79-31-2.